AWARD NUMBER: W81XWH-17-1-0139

TITLE: Development of a Novel Approach to Regenerate Functional Lungs

PRINCIPAL INVESTIGATOR: Munemasa Mori, M.D., Ph.D.

CONTRACTING ORGANIZATION: Columbia University Medical Center
New York, NY 10032

REPORT DATE: June 2019

TYPE OF REPORT: Final

PREPARED FOR: U.S. Army Medical Research and Materiel Command
Fort Detrick, Maryland 21702-5012

REPORT DOCUMENTATION PAGE

Form Approved
OMB No. 0704-0188

1. REPORT DATE	2. REPORT TYPE	3. DATES COVERED
June 2019	Final	1 May 2017 - 28 FEB 2019

4. TITLE AND SUBTITLE
Development of a Novel Approach to Regenerate Functional Lungs

5a. CONTRACT NUMBER

5b. GRANT NUMBER
W81XWH-17-1-0139

5c. PROGRAM ELEMENT NUMBER

6. AUTHOR(S)

Munemasa Mori, M.D., Ph.D.

E-Mail: mm4452@columbia.edu

5d. PROJECT NUMBER

5e. TASK NUMBER

5f. WORK UNIT NUMBER

7. PERFORMING ORGANIZATION NAME(S) AND ADDRESS(ES)

Columbia University (CUIMC)
650 West 168th Street
New York, NY 10032

8. PERFORMING ORGANIZATION REPORT NUMBER

9. SPONSORING / MONITORING AGENCY NAME(S) AND ADDRESS(ES)

U.S. Army Medical Research and Materiel Command
Fort Detrick, Maryland 21702-5012

10. SPONSOR/MONITOR'S ACRONYM(S)

11. SPONSOR/MONITOR'S REPORT NUMBER(S)

12. DISTRIBUTION / AVAILABILITY STATEMENT

Approved for Public Release; Distribution Unlimited

13. SUPPLEMENTARY NOTES

14. ABSTRACT Millions of people suffer from incurable refractory lung diseases. Currently, the only viable option for patients with end-stage pulmonary disease is lung transplantation. The discovery and development of novel treatments for refractory pulmonary disease therapies is relevant to public health, and to a few listed PRMRP Topics. To address this challenge, the main goal of this project was to regenerate functional lungs in vivo in rodents through a Blastocyst Complementation (BC) approach (Aim1), and *in utero* mediated progenitor transplantation as a contingency approach (Aim2). In this regard, we successfully generated functional lungs in mice via blastocyst complementation **(100% accomplishment)**. We injected normal donor pluripotent stem cells (PSCs) labeled by Enhanced Green fluorescent proteins (GFP) into recipient blastocysts harboring a lung agenesis phenotype. To generate a vacant organ niche specifically in the respiratory system, we utilized a novel approach, **Conditional Blastocyst Complementation** (CBC) via Fgfr2 genetic manipulation in the host embryos to avoid an undesired phenotype following injection of PSCs. To the best of our knowledge, we are the first to establish an approach for regeneration of fully functional lungs through CBC. We also established a method for efficient induction of authentic pluripotent stem cells (PSCs) that supported efficient generation of fully functional lungs. Using our authentic pluripotent stem cells (PSCs)-enriched culture condition, we rescued the lung agenesis phenotype of genetically deficient hosts via CBC. Notably, these pups survived throughout adulthood with normal lung function.

15. SUBJECT TERMS

16. SECURITY CLASSIFICATION OF:			17. LIMITATION OF ABSTRACT	18. NUMBER OF PAGES	19a. NAME OF RESPONSIBLE PERSON
a. REPORT	b. ABSTRACT	c. THIS PAGE			USAMRMC
Unclassified	Unclassified	Unclassified	Unclassified		19b. TELEPHONE NUMBER *(include area code)*

Table of Contents

Page

1. Introduction

This project focuses on the establishment of a novel experimental basis for lung regeneration in mice via blastocyst complementation (Aim1) and lung bud complementation (Aim2).

Millions of people suffer from incurable refractory lung diseases. Currently, the only viable option for patients with end-stage pulmonary disease is lung transplantation. However, there is a major shortage of donor lungs and there are no world reports of successful lung regeneration. The discovery and development of novel treatments for refractory pulmonary disease therapies is relevant to public health, and to a few listed PRMRP Topics. To address this challenge, the main goal of the original project was to regenerate functional lungs in vivo in rodents through a Blastocyst Complementation (BC) approach (Aim1), and *in utero* mediated progenitor transplantation as a contingency approach (Aim2). In this regard, we successfully generated functional lungs in mice via blastocyst complementation **(100% accomplishment)**. We injected normal donor pluripotent stem cells (PSCs) labeled by Enhanced Green fluorescent proteins (GFP) into recipient blastocysts harboring a lung agenesis phenotype. To generate a vacant organ niche specifically in the respiratory system, we utilized a novel approach, **Conditional Blastocyst Complementation** (CBC) via Fgfr2 genetic manipulation in the host embryos to avoid an undesired phenotype following injection of PSCs. To the best of our knowledge, we are the first to establish an approach for regeneration of fully functional lungs through CBC. We also established a method for efficient induction of authentic pluripotent stem cells (PSCs) that supported efficient generation of fully functional lungs. Using our authentic pluripotent stem cells (PSCs)-enriched culture condition, we rescued the lung agenesis phenotype of genetically deficient hosts via CBC. Notably, these pups survived throughout adulthood with normal lung function.

2. Keywords (limited to 20 words)

Blastocyst Complementation (BC)
Exogenous Progenitor Transplantation
Induced Pluripotent Stem Cells - (iPS) cells
In Utero Progenitor Injection
Lung Agenesis
Lung Bud Complementation (LBC)
Lung Generation
Lung Regeneration
Lung Tissue Engineering
Pluripotent Stem Cells (PSCs)

3. Accomplishments

The major goal of this research is to establish an experimental model for lung regeneration i*n vivo* as stated in the SOW.

List of goals as stated in the SOW and percentages of accomplishment

a. Selection of candidate genes for BC including characterization of lung agenesis mutant mice at Columbia University Medical Center (CUMC), NY.

We determined the frequency of *Shh* ^{Cre} *Fgfr2* $^{flox/flox}$ mutant embryos that developed lung agenesis and confirmed that the alleles/phenotypes followed Mendel's Law of Segregation by genotyping. We designed new sets of PCR probes. Briefly, we performed PCR using the following Tm-adjusted primers which allowed us to obtain equal band size in heterozygous allele: FR2-F1, ATAGGAGCAACAGGCGG, and FR2-F2, CAAGAGGCGACCAGTCA resulting in a 142 bp product for the wild-type allele and a 207 bp product for the conditional, floxed allele. A separate set of primers, FR2-F1 and FR2-F3, CATAGCACAGGCCAGGT were used to detect the locus following recombination by Cre recombinase (244 bp product). We further confirmed whether *Shh* ^{Cre} *Fgfr2* $^{flox/flox}$ mutant mice have additional phenotypes besides lung agenesis by lineage tracing mice *Shh* ^{Cre} *Fgfr2* $^{flox/flox}$; *Rosa* $^{tdtomato/+}$ mice (**See Fig. 1**). We characterized in detail their phenotypes by whole-mount immunostaining and immunohistochemistry (IHC) tissue sections (**See Fig. 2**).

Percent accomplished: 100%

b. Collection of embryos (E2.5) from each mutant mouse at CUMC, NY.

We performed superovulation with PMSG and hCG and harvested blastocysts (E2.5) under approved IACUC and ACURRO protocols. Cryopreservation of frozen embryos (E2.5) via simple vitrification methods was tested, but found inefficient in obtaining desired pups.

Percent accomplished: 100%

c. Perform BC (mouse GFP+ ES/iPS cells to mouse blastocysts) at CUMC, NY.

We maintained EGFP–expressing mouse pluripotent stem cells (PSCs). The best condition for pluripotent stem cells was determined by comparison with our previously defined cell culture system (**See Fig. 5**). Embryonic transfers in pseudo-pregnant mice were performed by CUMC's transgenic core, and post-transfer, we monitored the foster mothers. We sacrificed mice at appropriate days (P0) for preparation of frozen blocks and paraffin-embedded blocks, RNA samples were performed **(See Fig. 3, 4, 6-9)**.

Percent accomplished: 100%

d. Analyses of fixed tissues and embryos at CUMC, NY (Months 2-18): (See Fig. 3, 4, 6-9)

IHC analyses were performed during lung development and postnatal life in rescued mice (*Fgfr2*^{cunII} +GFP-PSC) as well as in control mice (*Fgfr2*^{cunII} +GFP-PSC). We performed morphometric analyses on lung epithelial cell types such as alveolar type1, type2 cells, ciliated, and secretory cells by confocal microscopy analysis.

Percent accomplished: 100%

e. Preparation of progress report and manuscript, CUMC, NY (Months 15-18).

Results from experiments proposed in Aim 1 have been assembled in a manuscript and submitted to "*Science*". The editor has requested a resubmission of a revised version of the manuscript once the criticisms have been addressed.

Percent accomplishment: 100%

Summary of ACCOMPLISHMENTS in Aim1:

Studies during the initial period of funding were focused on Aim 1. The goals of this Aim are to establish an experimental model for lung regeneration via blastocyst complementation (BC). As explained in our proposal, initiation of lung organogenesis is crucially dependent on the local activation of Fgfr2 signaling in the foregut endoderm by its ligand *Fgf10* in the mesoderm. Fgf10-Fgfr2 signaling expands early lung progenitors to form primordial lung buds. Depletion of *Fgfr2* or *Fgf10* in mice does not prevent the trachea from forming but leads to lung agenesis (*1–3*). Importantly, *Fgfr2*-mediated MAPK signaling is similarly required in developing structures, such as the limbs and during early embryogenesis, is critical for trophoblast formation(*1–4*). The preliminary data described in this application showed the lung agenesis phenotype that resulted from endodermal disruption of Fgfr2 (*Shh*$^{cre/+}$*Fgfr2*$^{f/f}$, hereafter, *Fgfr2*^{cnull}).

Work during the initial year of funding confirmed that the alleles/phenotypes followed Mendel's Law of Segregation. We also confirmed that Shh-lineage traced cells in these mutant mice do not exhibit morphological defects in the placenta, limbs and brain other than lung agenesis phenotypes (**Fig. 1 and Fig. 2**). The placenta was not labeled by tdTomato, but limbs, lungs and brains in *Fgfr2*^{hetero}*;Rosa*$^{tdTomato/+}$ were specifically labeled by tdTomato (Fig. 1). Importantly, lung signals could not be detected in *Fgfr2*^{hetero} *Fgfr2*^{cnull} *pups,* while no gross defects were noted in the limbs and brain. To prevent undesired multi-organ phenotypes not amenable to rescue by BC, we coupled BC with a conditional gene-ablation strategy to vacate a specific niche in the host for targeted complementation (CBC, or conditional blastocyst complementation). Thus, we used these conditional *Fgfr2* knockout mice (*Fgfr2*^{cnull}) to inactivate Fgfr2 in the foregut endoderm immediately prior to the onset of lung organogenesis (*5*, *6*). Analysis of E13.5 *Fgfr2*^{cnull} embryos showed lung agenesis with preserved trachea and esophagus (Sox2+Nkx2-1+ and Sox2+, respectively) (Fig. 2A-B) (*1*). We found no placental defects in *Fgfr2*^{cnull} and the mice died at birth (*7*, *8*). As an initial attempt to complement a defective organ niche in *Fgfr2*^{cnull} mutants, we used pluripotent stem cells (PSCs) derived from an *Nkx2-1-GFP knockin* mouse as donor cells PSC$^{Nkx2\text{-}1\text{-}GFP}$

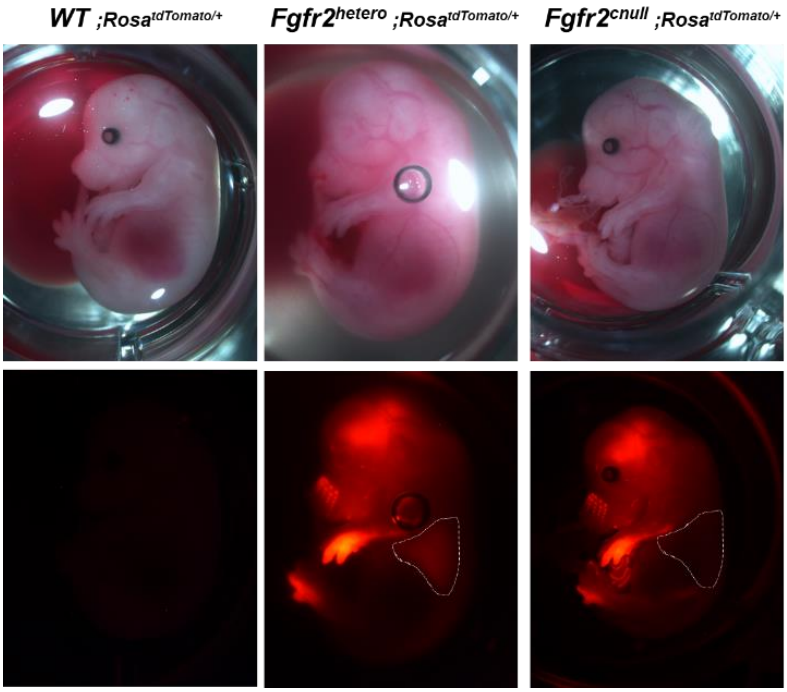

Fig. 1 Lung specific phenotype in Shh-lineage tracing mice: Shh-lineage traced cells (tdTomato: Red) were labeled. Fgfr2 heterozygous conditional allele (*Fgfr2* ^{hetero}*;Rosa* $^{tdtomato/+}$) could obtain lungs, but not homozygous allele (*Fgfr2* ^{cnull}*;Rosa* $^{tdtomato/+}$).

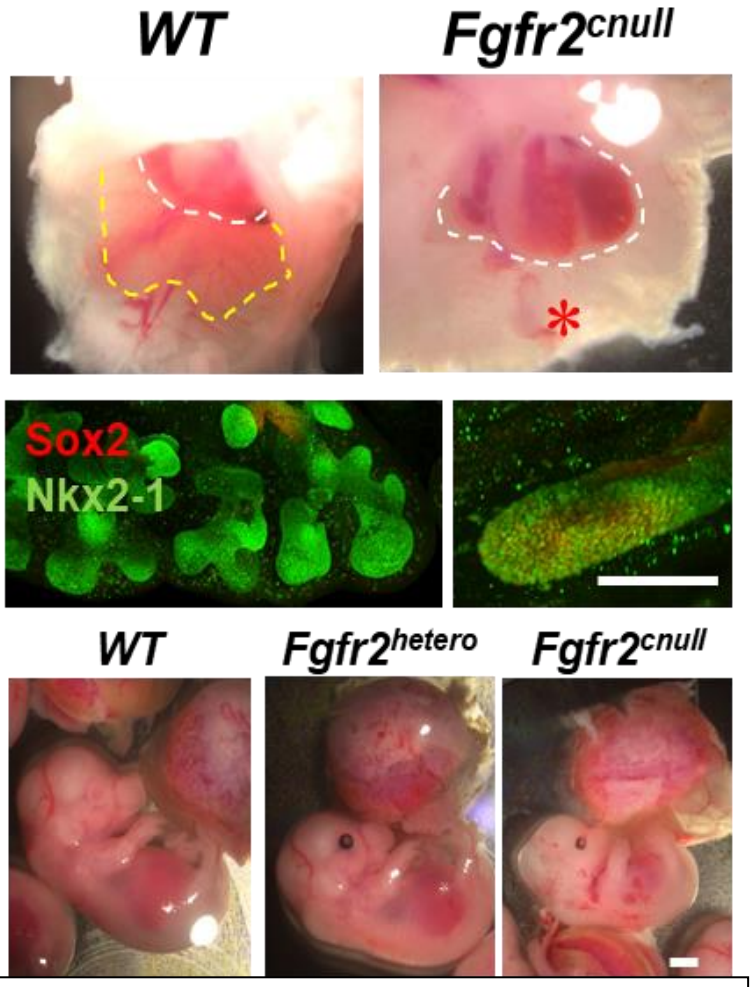

Fig. 2 Lung agenesis phenotype in Fgfr2 mutant mice . Reproducible lung agenesis phenotype in Fgfr2 ^{cnull} without any morphological defects in placenta and limbs. In Fgfr2 ^{cnull} mice, Sox2 + proximal tracheal airway lineages were preserved.

cultured in 2i-media condition (*9*). These cells express green fluorescent protein (GFP) from the *Nkx2-1* locus, thus marking all lung epithelial progenitors from their earliest stages. PSCs$^{Nkx2\text{-}1\text{-}GFP}$ were expected to respond to Fgf10 from the host to form the lungs (*10*). Among the 25 PSCs$^{Nkx2\text{-}1\text{-}GFP}$ injected into *Fgfr2*^{cnull}, WT or *Fgfr2* ^{hetero} blastocysts transferred to pseudo-pregnant mothers, 12 reached term. Of these, two showed respiratory distress, dying immediately at birth. The remaining 10 pups were sacrificed as 2-month old adults. Analysis of their lungs showed chimerism in 5 of these mice; GFP signals were nevertheless patchy and low, suggesting that the niche to be complemented was unlikely vacant as expected in *Fgfr2*^{cnull} mutants. Surprisingly, in embryos that died at birth, instead of agenesis, GFP+ donor-derived lungs were present in the thoracic cavity. Although uninflated and thus slightly smaller, these lungs had no obvious gross abnormalities suggestive of altered lobation or arrested branching morphogenesis (Fig.3). Morphometric analyses revealed that nearly 100% of the lung epithelium was comprised of GFP+ cells. The extensive overlap of GFP and nuclear Nkx2-1 signals further confirmed that PSCs$^{Nkx2\text{-}1\text{-}GFP}$ were able to complement with high efficiency a vacant endodermal niche in the *Fgfr2*^{cnull} hosts to undergo lung organogenesis (Fig.3, 4). Nevertheless, the chimeric lungs were

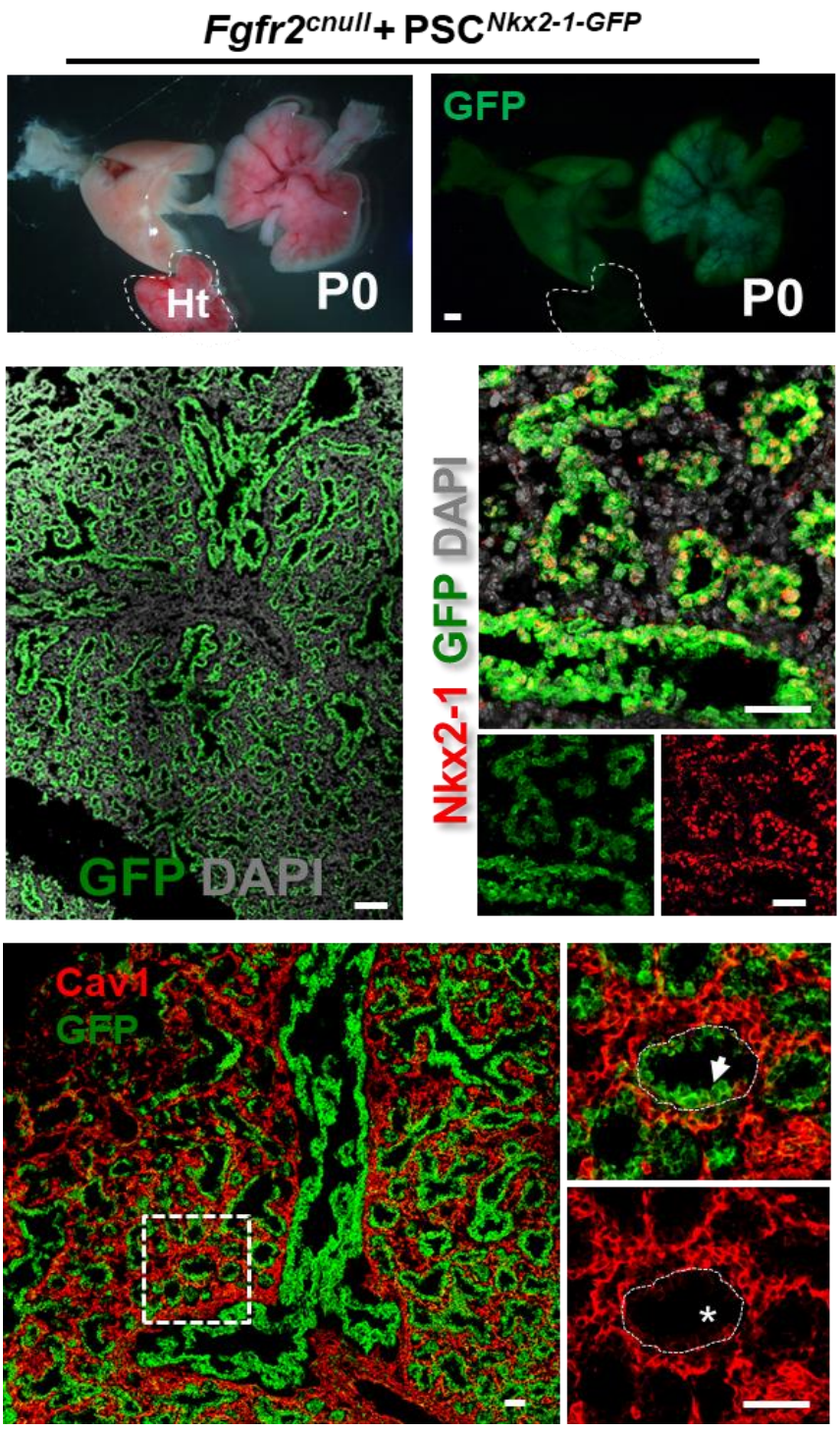

Fig. 3 Rescue of lung agenesis phenotype by CBC. Newborn (P0) *Fgfr2cnull* mice complemented by PSC $^{Nkx2\text{-}1\text{-}GFP}$. Macroscopic view (top): GFP signals in lungs not in heart (Ht). GFP double-labeling with Nkx2-1, but not with Caveolin1 (*) in the lung epithelium.

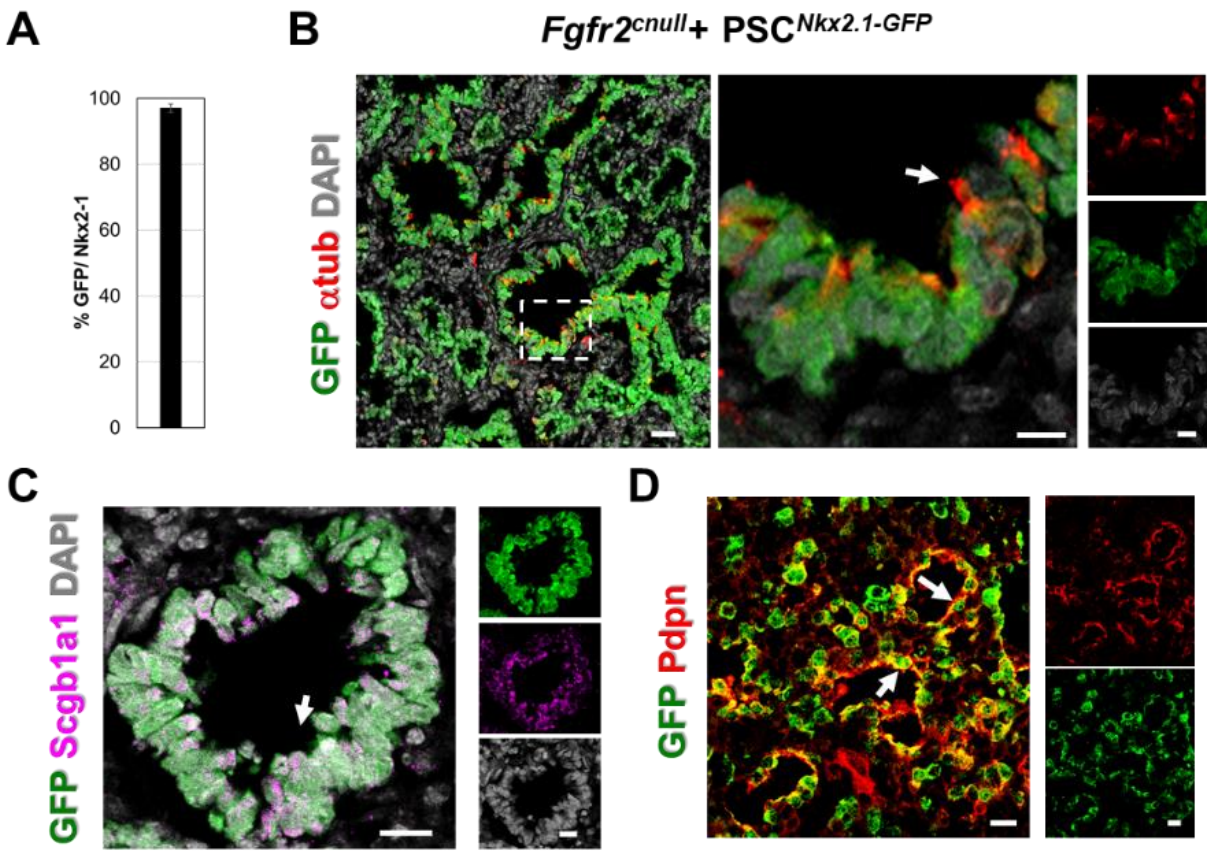

Fig.4 ***Fgfr2cnull*** **+ PSCNkx2-1-GFP newborn lungs**. (**A**) Percent of GFP+ cells in the airway epithelium (Graph: mean + se) in 5-random fields per sample (N=2). (**B-D)** Immunofluorescence of GFP, acetylated a-tubulin (**B**), Scgb1a1 (**C**) and Pdpn (**D**) (arrows: 5 double-labeled ciliated, secretory or alveolar type1-like cells). Lateral panels: single channels or high magnification images. Scale bars: B-D= 10 µm

immature. Airways branched and differentiated seemingly normally, but the alveolar saccules crucial for gas-exchange never formed. Cuboidal Sftpc-expressing cells (putatively alveolar type 2) and Pdpn-labelled type 1 (AT1) cells were seen in these lungs, but Caveolin1 is nearly absent in the distal epithelium, albeit Caveolin1 is widespread in the distal mesenchyme suggesting that AT1 cell differentiation did not occur (Fig. 3, 4). Thus, complementation with PSCs$^{Nkx2\text{-}1\text{-}GFP}$ was inefficient in carrying out the final steps of lung maturation and functionally rescuing the respiratory failure of *Fgfr2*^{cnull} hosts. We reasoned this could have resulted from low developmental potential of PSCs$^{Nkx2\text{-}1\text{-}GFP}$ perhaps due to the Nkx2-1 haploinsufficiency of this knockin line and/or a non-optimal protocol used to maintain these cells in culture (*11–13*). Analyses of different PSC lines and protocols for CBC optimization identified PSCs$^{CAG\text{-}GFP}$ as highly efficient donor cells. This line carries a GFP transgene under the CMV enhancer-chicken β-actin promoter (CAGGS) for ubiquitous tissue expression. A systematic comparison of culture conditions for optimal maintenance of pluripotency showed that the treatment of PSCs$^{CAG\text{-}GFP}$ with LIF/VPA yielded a relatively high SSEA1 expression together with a decent amount of Oct4 expression among the defined pluripotency maintenance media tested here (Fig. 5) (*9*, *11*, *12*, *14*, *15*). SSEA-1 expression in the donor PSCs is closely correlated with efficient chimera formation, even in the later developmental stages of mouse embryos (*16*). Therefore, PSCs$^{CAG\text{-}GFP}$ treated with LIF/VPA for 5 days were injected into *Fgfr2* mutant blastocysts and transferred to pseudo-pregnant recipient mice as before. Offspring were analyzed at birth (P0: postnatal day) for evidence of rescue of neonatal respiratory failure and survival. Among the 24 pups obtained, only one died at birth and was found to have lung agenesis of non-complemented *Fgfr2*^{cnull} mice. All others were active and moved around without signs of respiratory distress. 16 animals showed strong GFP in the skin, while the remaining 7 had low to undetectable expression. Although, based on GFP expression, skin chimerism appeared similar in all pups regardless of the phenotype, the dissected lungs from PSCs$^{CAG\text{-}GFP}$-complemented *Fgfr2*^{cnull} animals showed the strongest GFP signals (Fig.6). Normal activity, feeding

behavior and respiratory frequency rates of PSCs$^{CAG-GFP}$-complemented *Fgfr2*^{cnull} mice and the widespread distribution of air-bubbles, without areas of atelectasis was consistent with the rescue of a fully functional neonatal lung. Histological analysis confirmed that GFP expression in the lungs increased from WT, *Fgfr2*^{hetero} and *Fgfr2*^{cnull} mice, suggestive of more efficient CBC complementation with a decreased Fgfr2 gene dose of the host (Fig. 6). More GFP+ cells double-labeled with epithelial markers of differentiation were present in lungs from mice carrying less Fgfr2 gene copies, as exemplified by Pdpn, a marker of type I cells. Immunofluorescence analyses showed GFP staining overlapping with markers of the key epithelial cell types in the alveolar (type 1 and 2) and airway (secretory Club, multiciliated and neuroendocrine) compartments (Fig. 7). Remarkably, the frequency of Pdpn+, Sftpc+, Scgb1a1+, β4 Tubulin+ or Sox2+(marker of airway progenitors) cells double-labeled with GFP increased from 20-30% in WT lungs to nearly 100% in *Fgfr2*^{cnull} in CBC-complemented lungs (Fig. 7E). Interestingly, in PSCs$^{CAG-GFP}$ + *Fgfr2*^{cnull} animals, the

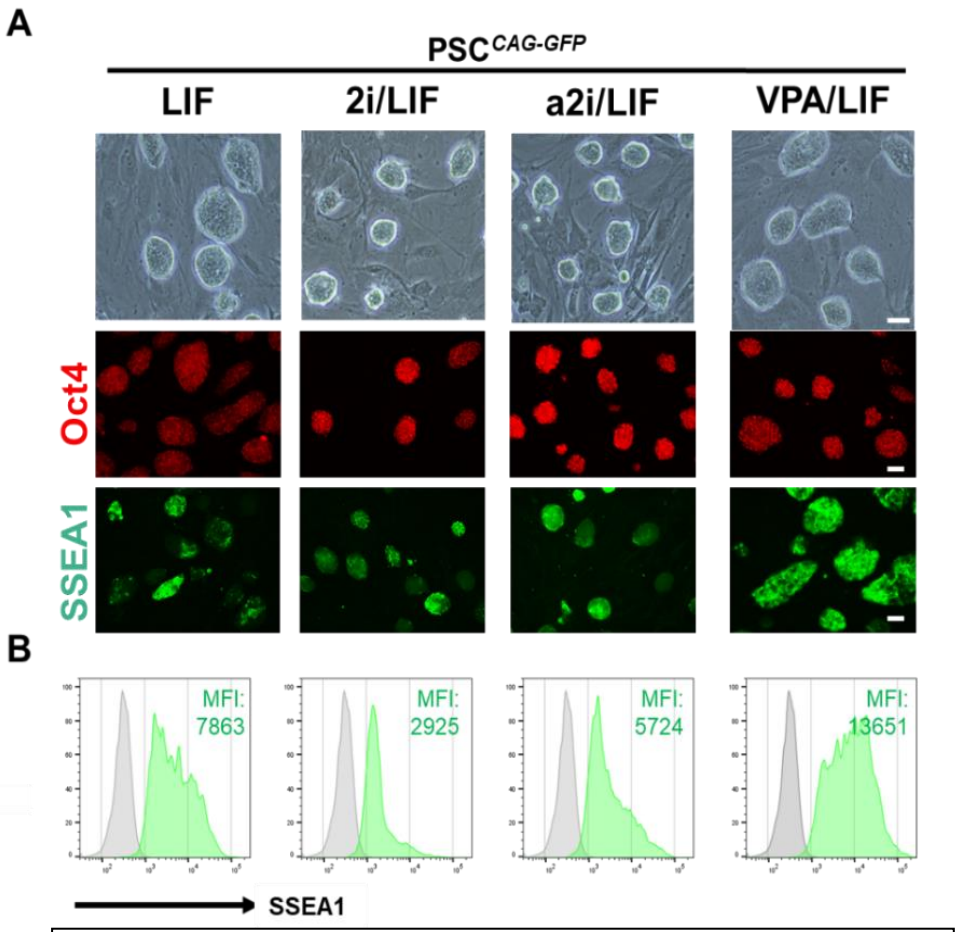

Fig.5 Representative morphology and pluripotency markers (Oct4 and SSEA1) in each defined culture condition. Representative morphology of PSC$^{CAG-GFP}$ colonies on MEFs (**A**), and its representative profiles of pluripotency markers (Oct4 and SSEA1) under the several culture conditions. (B) Histograms by flow cytometry analyses confirmed the relatively enhanced expression of SSEA1 in live PSC$^{CAG-GFP}$ cells cultured in VPA/LIF 5 condition. Scale bars: A= 10 µm

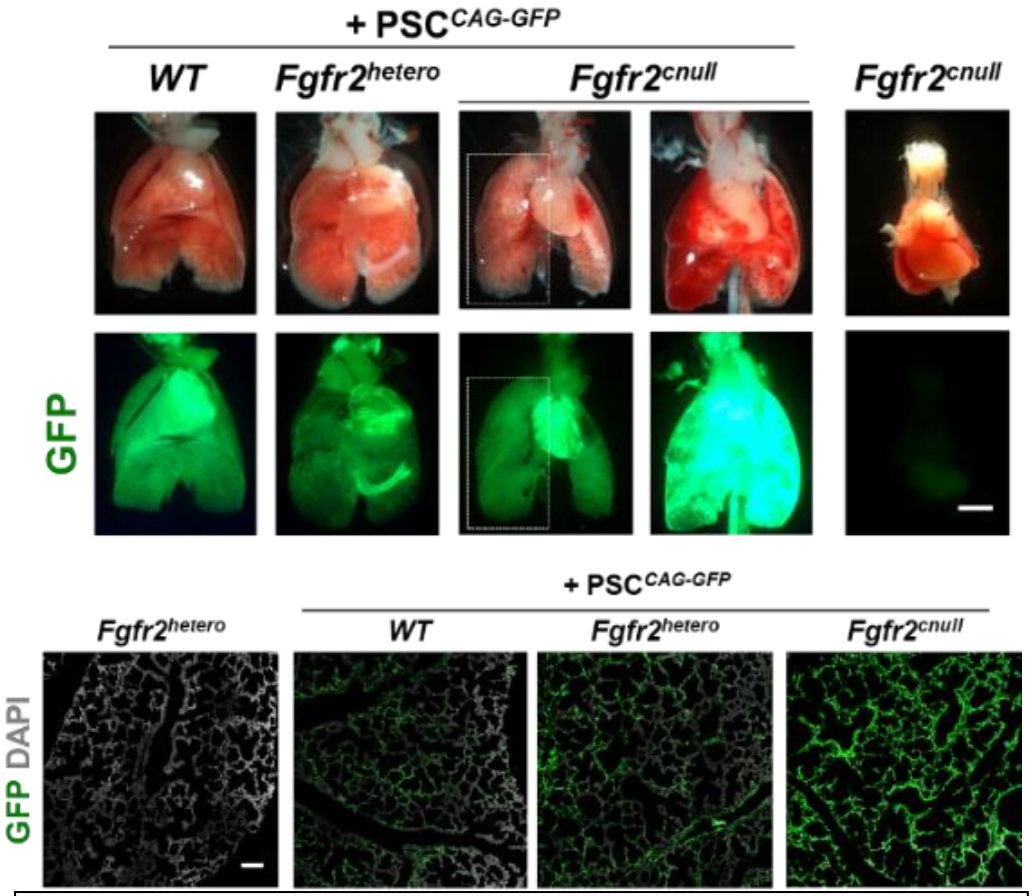

Fig. 6 Rescued lung agenesis phenotype in Fgfr2 ^{cnull} mice by blastocyst complementation: whole mount freshly isolated newborn lungs with neighbor structures showing GFP signals (bottom) in WT*, Fgfr2^{hetero} and Fgfr2 ^{cnull}* injected with PSCCAG-GFP cells. (B) Histological sections from the lungs above (*Fgfr2^{hetero}* GFP- as control). Scale bars: top panel, bottom panel, =1mm, 20µm, respectively

frequency of GFP+ cells (%GFP/DAPI) in the lung was significantly higher (~80%) than in the trachea or extrapulmonary airways (Fig. 8). This supports the idea that lung agenesis and preserved trachea in *Fgfr2^{cnull}* hosts provided different opportunities for CBC complementation even within the same organ. No consistent difference in chimerism was detected in lung mesenchymal derivatives (endothelium, airway or vascular smooth muscle) when *WT*, *Fgfr2^{hetero} or Fgfr2^{cnull}* chimeric lungs were compared (Fig. 8). The rare smooth muscle cells

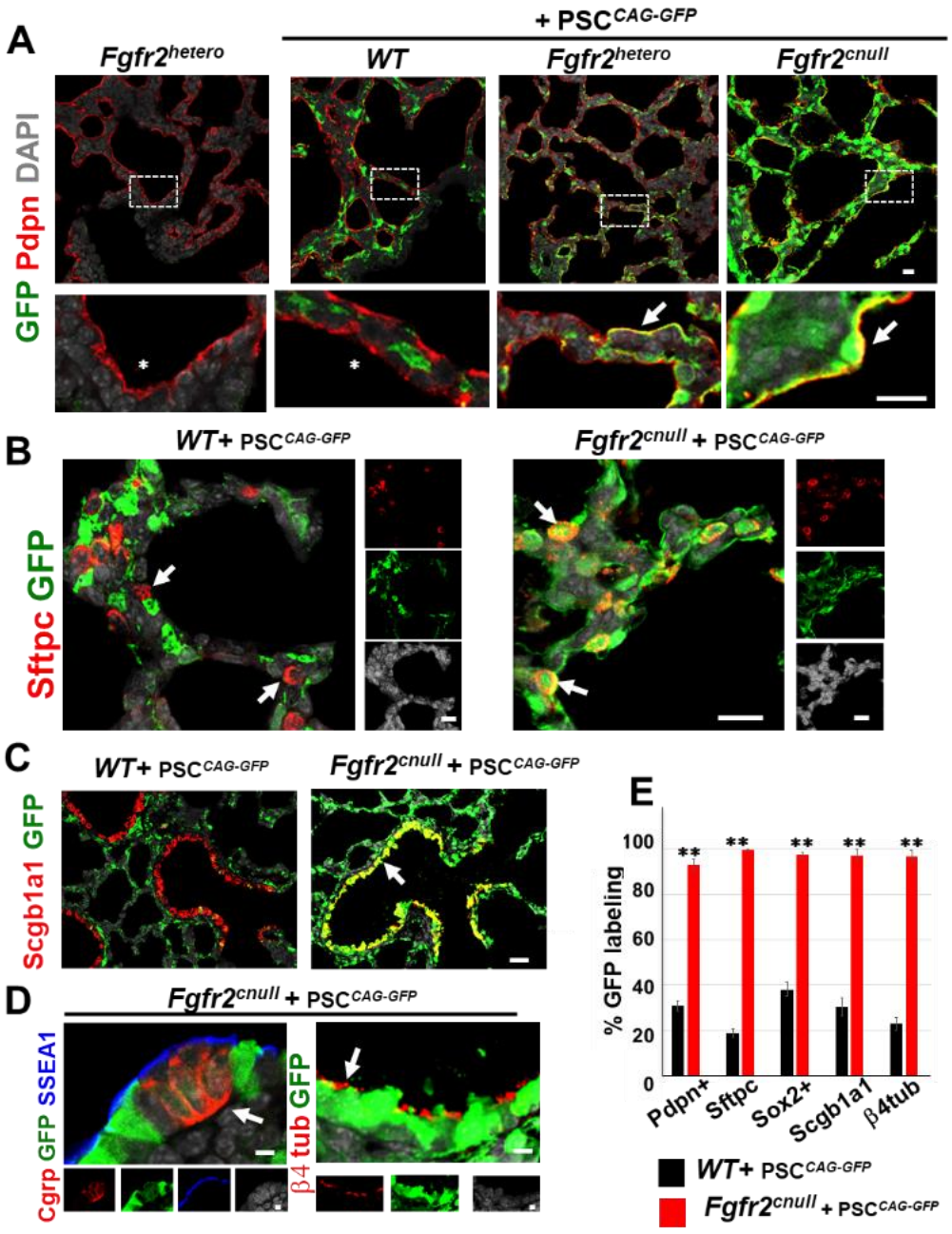

Fig. 7 M**arker analysis of PSCCAG-GFP-complemented lungs of *Fgfr2* mutants (A-D)** Immunofluorescence and confocal microscopy in lung sections of P0 mice showing expression of GFP and markers for alveolar type 1 (Pdpn), type 2 (S 5 ftpc), secretory (Scgb1a1), neuroendocrine (Cgrp), and multiciliated (b4 tubulin) cells. Bottom panels in (A): boxed areas enlarged from top panels; arrows in A, B: GFP+marker+ cells (*: marker+ alone). (**E**) Percentage of GFP associated with each marker in P0 *WT*+ PSCCAG-GFP or *Fgfr2cnull*+ PSCCAG-GFP mice. Graph: mean±s.e.m. in 10 random fields per sample. Student's t-test, **P<0.01. Scale bars: A, B, C, D=5, 10, 20, 5µm, respectively.

labeled with GFP were not preferentially associated with arteries, veins or airways of complemented lungs. Analysis of other organs showed negligible liver chimerism across phenotypes (Fig. 9). Rare scattered GFP+ cells were present in sections of adult liver and kidneys of *Fgfr2*^{cnull} + PSC$^{CAG-GFP}$. Although GFP+ cells were more abundant in the intestine, quantitative analysis showed no significant difference in labeling between WT and *Fgfr2*^{cnull} animals (Fig. 9).

However, VPA/LIF-treated PSCs had limited ability to form chimeras (~ 33-67%) efficiently. Moreover, VPA/LIF + PSCs$^{CAG\text{-}GFP}$ *Fgfr2^{cnull}* complemented embryos displaying low GFP signals in the skin or other internal organs often showed partial lung complementation, suggestive of the lower frequency in reaching in the host lung niche (Table 1, Fig. 10c).

Table 1. Summary of the survival rate and chimera rate in various experimental conditions.

Cell line	# Passage	Donor PSC background	PSC treatment	# Host blastocysts	Host blastocyst background	# injected PSCs/ blastocyst	% survival (# pups or embryos/ # transferred blastocysts)	% chimera formation*
PSC$^{Nkx2\text{-}1\text{-}GFP}$	15	W4/129S6	2i/LIF	25	129xB6xCD1	10	40% (10 neonates at P0)	50% (5 chimeras)
ES1$^{CAG\text{-}tdTomato}$	12	C57BL/6N	LIF	40	129xB6xCD1	10	40% (10 neonates at P0)	10% (1 chimera)
ES1$^{CAG\text{-}tdTomato}$	14	C57BL/6N	LIF	25	129xB6xCD1	10	24% (6 neonates at P0)	33% (2 chimeras)
ES1$^{CAG\text{-}tdTomato}$	14	C57BL/6N	a2i/LIF	30	129xB6xCD1	10	23% (7 neonates at P0)	71.4% (5 chimeras)
PSC$^{CAG\text{-}GFP}$	10	F1 hybrid mouse (C57Bl/6 x129)	LIF/VPA	43	129xB6xCD1	20	53.5% (23 neonates at P0)	66.6% (15 chimeras)
PSC$^{CAG\text{-}GFP}$	10	F1 hybrid mouse (C57Bl/6 x129)	LIF/VPA	12	129xB6xCD1	20	53.5% (6 embryos at E15.5)	88% (5 chimeras)
PSC$^{CAG\text{-}GFP}$	10	F1 hybrid mouse (C57Bl/6 x129)	LIF/VPA	40	129xB6xCD1	20	38% (15 neonates at P0)	33.3% (5 chimeras)
PSC$^{CAG\text{-}GFP}$	11	F1 hybrid mouse (C57Bl/6 x129)	a2i/VPA/LIF	43	B6	20	47% (20 neonates at P0)	85% (17 chimeras)
PSC$^{CAG\text{-}GFP}$	11	F1 hybrid mouse (C57Bl/6 x129)	a2i/VPA/LIF	40	129xB6xCD1	20	50% (20 neonates at P0)	64.2% (13 chimeras)
PSC$^{CAG\text{-}GFP}$	11	F1 hybrid mouse (C57Bl/6 x129)	a2i/VPA/LIF	87	B6	20	35.6% (31 neonates at P0)	65.2% (20 chimeras)
PSC$^{CAG\text{-}GFP}$	11	F1 hybrid mouse (C57Bl/6 x129)	a2i/VPA/LIF	18	129xB6xCD1	20	50% (9 embryos at E12.5)	100% (9 chimeras at E12.5)
PSC$^{CAG\text{-}GFP}$	13	F1 hybrid mouse (C57Bl/6 x129)	a2i/VPA/LIF	80	129xB6xCD1	20	25% (20 neonates at P0)	70% (14 chimeras)
PSC$^{CAG\text{-}GFP}$	11	F1 hybrid mouse (C57Bl/6 x129)	a2i/VPA/LIF	36	129xB6xCD1	20	44% (16 embryos at E15.5)	100% (16 chimeras at E15.5)
PSC$^{CAG\text{-}GFP}$	11	F1 hybrid mouse (C57Bl/6 x129)	a2i/VPA/LIF	51	129xB6xCD1	20	50% (26 neonates at P0)	88.9% (23 chimeras)
PSC$^{CAG\text{-}GFP}$	11	F1 hybrid mouse (C57Bl/6 x129)	a2i/VPA/LIF	35	129xB6xCD1	20	43% (15 neonates at P0)	100% (15 chimeras)
FL19 ARR3-1	11	C57BL/6N	a2i/VPA/LIF	20	C57BL/6J	10	60% (12 neonates at P0)	100% (12 chimeras)
FL19 ARR3-2	11	C57BL/6N	a2i/VPA/LIF	20	C57BL/6J	10	40% (8 neonates at P0)	100% (8 chimeras)
B7	15	C57BL/6N	2i/LIF	40	CD1	10	33% (13 neonates at P0)	62% (8 chimeras)
SUN107.4	16	CD1	2i/LIF	20	CD1	8	30% (6 neonates at P0)	50% (3 chimeras)

N.A.: Not applicable for complementation analyses, since host embryos were WT.

* Based on the chimerism in the skin of postnatal day0 neonates.

Since VPA was key in improving chimera formation (*14*, *17*), we assessed the additive effect of VPA in each culture condition to identify the most efficient induction of pluripotency markers and the ability to sustain chimeras throughout development. We found that, while VPA/LIF and a2i/VPA/LIF were equally efficient in generating the highest proportion of the $SSEA^{high}$ $PECAM^{+}$ $PSC^{CAG\text{-}GFP}$ population, Oct4 levels were significantly higher in a2i/VPA/LIF cultures (Fig. 10a-b). In a2i (alternative 2i) medium the MEK kinase inhibitor is replaced by an Src kinase inhibitor (CGP77675) known to enhance PSC germline competency and developmental potential (*11*, *12*). When injected into *WT* blastocysts, donor a2i/VPA/LIF-treated $PSCs^{CAG\text{-}GFP}$ nearly maximized the ability to form chimeras among all conditions tested (Fig. 10c-d; Table1). We further confirmed that a2i/VPA/LIF PSCs population forming the highest chimera rate at birth was the $SSEA1^{high}$ PSCs, but not $SSEA1^{dim}$ when isolated by FACS (Fig. 11a). We then tested whether this population of $SSEA1^{high}$ PSCs would allow CBC generated lungs to be fully functional throughout life in genetically deficient hosts.

We used two distinct mouse models of agenesis as a host: the former $Fgfr2^{cnull}$, in which tracheal and lung progenitors are specified, but the lung progenitors are selectively unable to expand, and the $Ctnnb1^{cnull}$ ($Shh^{cre/+}Ctnnb1^{f/f}$) in which none of these progenitors are specified and thus neither lung nor trachea form (*18*). These enabled us to assess whether targeting different genes crucial for the respiratory organogenesis under the same CBC strategy allowed rescuing these structures as expected.

Remarkably, all chimeric animals with lung complementation developed normally to adulthood and reached full maturity. As a collaborative work with Dr. Jennifer A. Danielsson and Dr. Charles W. Emala, we performed pulmonary function tests (Flexivent) in adult mice to assess the values of airway resistance, lung elastance, and compliance comparable to WT littermates. Importantly, when challenged with a spasmogenic agent (methacholine) CBC-complemented lungs showed a concentration-dependent bronchoconstriction response indistinguishable from controls (Fig. 11b, 3c). Macroscopic analysis of $Ctnnb1^{cnull}$ $+PSC^{CAG\text{-}GFP}$ mice showed strong GFP signals in the trachea and lungs suggesting efficient donor complementation in all respiratory progenitors (Fig. 12). In $Fgfr2^{cnull}$ $+PSC^{CAG\text{-}GFP}$ complementation occurred preferentially in the lung, compared to the trachea (Fig. 8a, 11c). Immunofluorescence of lungs from $Fgfr2^{cnull}$ $+PSC^{CAG\text{-}GFP}$ and $Ctnnb1^{cnull}$ $+PSC^{CAG\text{-}GFP}$ showed extensive GFP overlap with markers of the airway and alveolar epithelial cell types (Fig. 11c).

In summary, we established a conditional gene-ablation strategy to vacate a specific niche for targeted complementation (CBC) coupled with a novel methodology for enhancing the PSCs' chimerization and developmental potential. These procedures were used to overcome significant hurdles to generate lung and trachea in the context of a severe genetic defect that impaired organ development. The approach took advantage of bona fide tissue interactions in vivo in chimeric embryos to form complemented lungs in hosts that lived to adulthood. To the best of our knowledge, this is the first evidence of regeneration of defective respiratory progenitor niches allowing the formation of fully functional lungs in vivo. The different PSCs and genetically altered hosts used here suggest that our approach is versatile and can be applied to other organs. Our work lays a foundation for conceptual and technical platforms for investigating mechanisms of cell competition during mammalian organogenesis or as part of the surveillance mechanisms that maintain tissue integrity essential for homeostasis and regeneration-repair. Lastly, our observations open perspectives for the use of CBC in the engineering of complex organs in large animals and ultimately in cell-based interventions for regenerative purposes in human conditions.

We have submitted to Nature Medicine our report on the first, generation of functional lungs in vivo. Our findings are currently under review.

Aim 2: Regeneration of lungs via in utero injection in mice

Accomplishment status along SOW

a. Preparation of materials and reagents for in utero injection, CUMC, NY (Months 3-12).

We first tested whether we could target lungs by ultrasound echo technically assisted by Dr. Ellen Ezratty and her lab members (CUMC, NY). We could not identify the lung buds at E9.5.

Percent accomplished: 5%

b. Preparation of mouse/human ES/iPS cells or new mouse lines at CUMC, NY.

We selected mouse ES cell lines and culture conditions for the highest efficient chimerism, an essential feature for the evaluation of pluripotency (**Fig. 5**).

Percent accomplished: 30%

c. Injection of mouse/human ES/iPS cells in mouse embryos (E9.5~E11.5) under guidance of photoacoustic/ultrasound echo with nanoparticles at CUMC, NY and/or Sloan Kettering Cancer center, NY.

An initial attempt using ultrasound echo to target the embryonic lung at early stages was unsuccessful. We found that it is difficult to identify mouse lung buds at E9.5~E11 even under high-frequency ultrasound echo guidance. Therefore, we realized injecting lung progenitors at a later time point of mouse development (around E11.5~E16.5) before and after thymus formation or using large animal model would be the ideal.

Percent accomplished: 30%

Summary of ACCOMPLISHMENTS in Aim2: Because we were successful in achieving goals highlighted in Aim1 and studies in Aim2 were proposed mostly as a contingency strategy, our efforts were primarily concentrated on Aim1. Additionally, new and revised experiments were required for *Science and Nature Medicine* (Fig. 10-12). For studies targeting the embryonic lungs intrauterinally, we teamed up with Dr. Ellen Ezratty (CUMC, NY) to use an ultrasound echo approach and localize the potential sites of injection of PSC in the early developing lung. However, as initially proposed, we were not able to identify the lung buds at E9.5 under high-frequency ultrasound echo. Therefore, we tested later time points of mouse development (E11.5~E16.5) as alternative options for this approach. We did undertake efforts to generate mice expressing iRFP in the Rosa26 locus, but felt that our efforts were better directed to concentrate on Aim1 as described above.

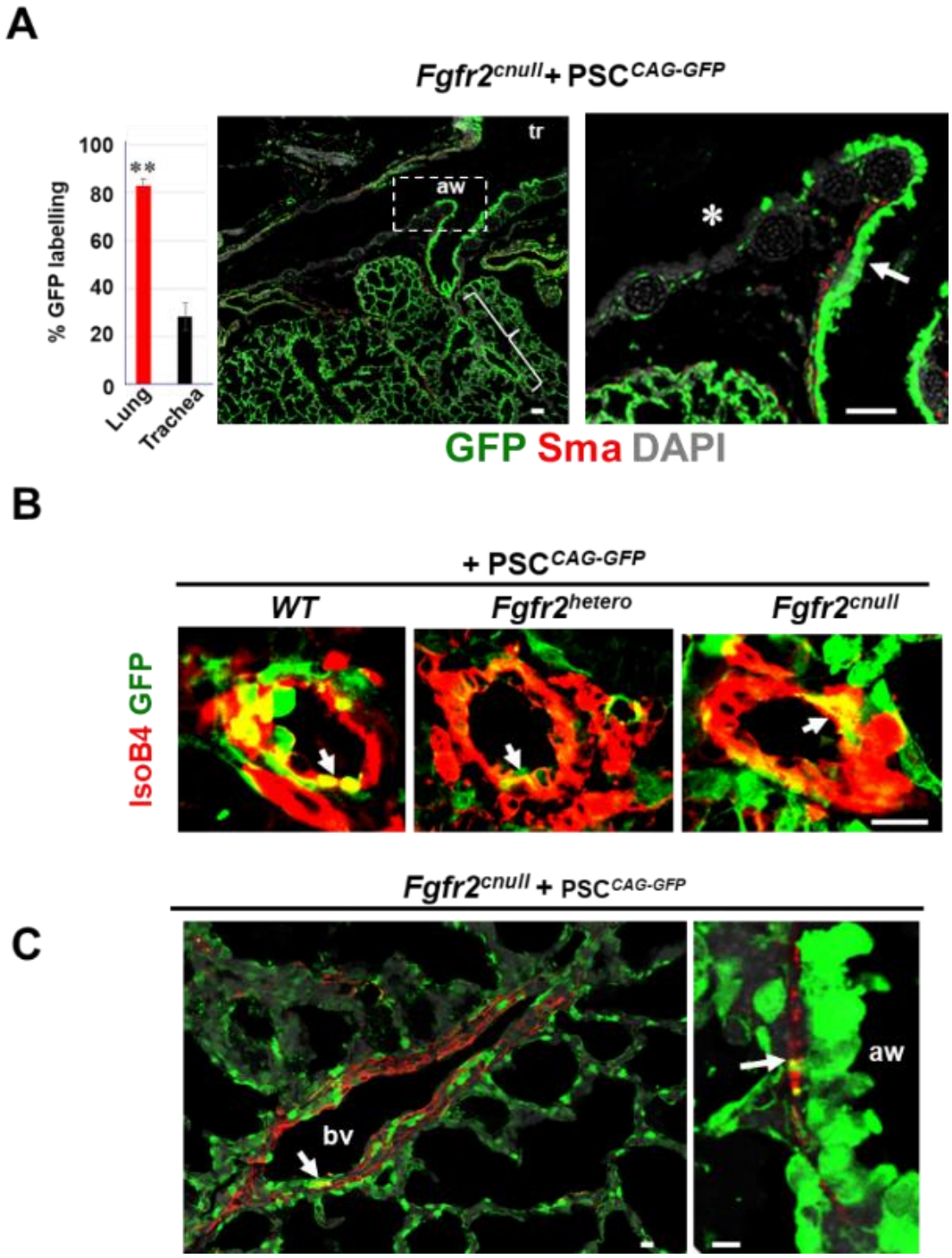

Fig. 8 Representative image of vasculatures and lung mesenchyme in chimeric lungs (**A)** GFP-Isolectin B4 double-labeled endothelial cells (arrow) in P0 *WT*+ PSCCAG-GFP and *Fgfr2cnull*+PSCCAG-GFP chimeric lungs. (**B**) GFP-Sma double-labeling of smooth muscle cells (arrow) in blood vessels (bv) and airways (aw) in P0 lungs from PSCCAG-GFP complemented *Fgfr2cnull* mice. Scale bars: A, B, = 10μm, 5μm.

Impact:
Millions of people worldwide suffer from incurable lung diseases. Currently, the only viable option for patients with end-stage pulmonary disease is lung transplantation. However, there is a major shortage of donor lungs and there are no world reports of successful lung regeneration. Notably, we successfully accomplished lung regeneration in vivo by the methods described in Aim1. Our experimental accomplishments will provide the foundation for advancing studies to large animal models, such as pigs and sheep to convert from basic research to translational research for refractory lung diseases in the near future. Our accomplishment will open an avenue for a personalized/precision medicine approach to tissue engineering using autologous cellular therapies. BC technology and in utero injection of pluripotent stem cells (iPS) can potentially advance the field of regenerative medicine. The success of our studies can ultimately change the criteria for operable lung transplantations for refractory lung diseases. Therefore, we propose this novel approach as a next generation of promising therapy for refractory lung diseases.

What opportunities for training and professional development has the project provided?
Nothing to report.

How were the results disseminated to communities of interest?
This final report follows a previously filed progress report. A submitted manuscript is currently in the final revision stage and will be submitted for publication.

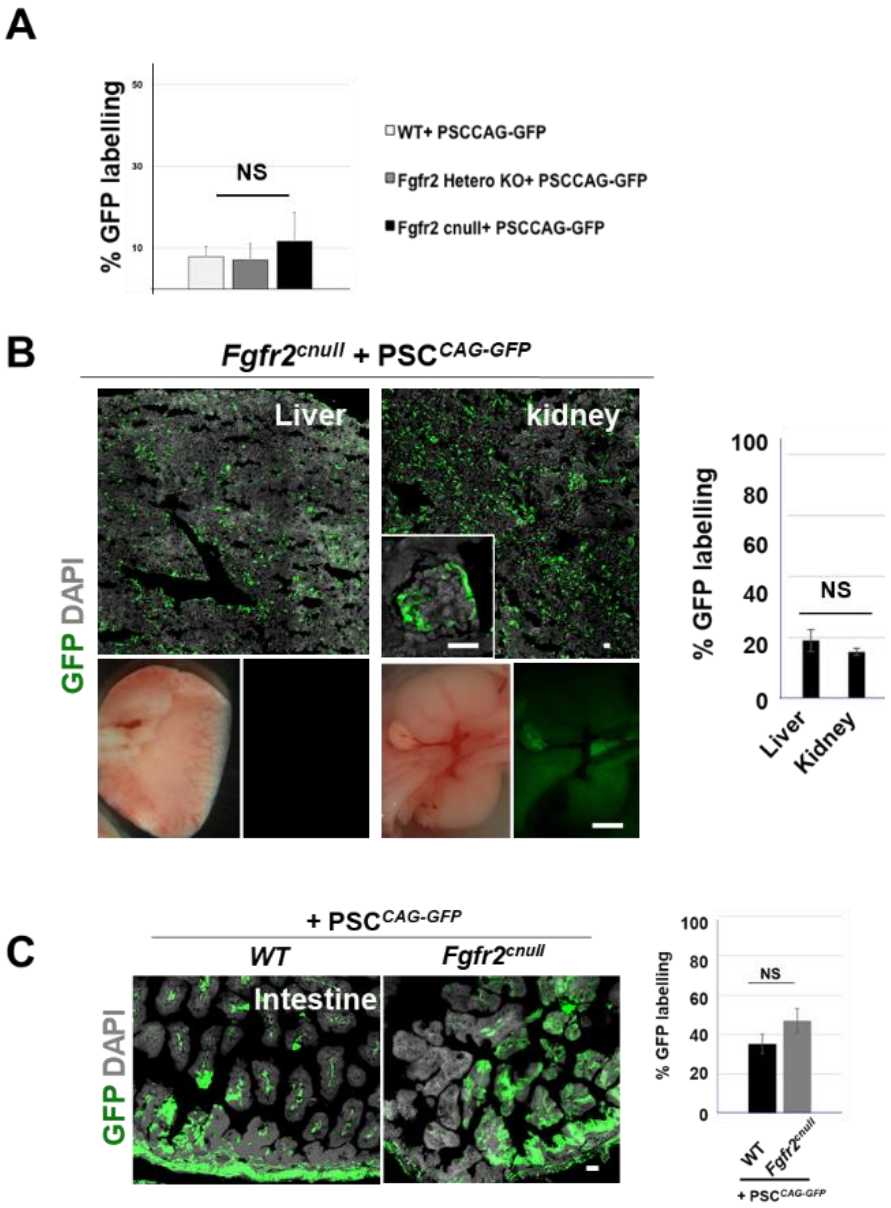

Fig. 9 Chimerism in other organs: Chimerism analyses in other organs **(A)** Statistical analyses: percentage of GFP+ cells analyzed by flow cytometry in the liver tissue from newborns (P0) or embryos (E15.5) in each pup of WT, *Fgfr2hetero or Fgfr2cnull* injected with PSCCAG-GFP cells: mean±s.e.m. in each condition. Student's t-test (NS: non-significant) 5 **(B)** GFP expression in whole mount and histological sections of *Fgfr2cnull +* PSC*CAG-GFP* liver and kidney; graph: mean±s.e.m. in 5random fields per sample. Student's t-test (NS: non-significant). (**C**) GFP expression in intestine from WT *or Fgfr2cnull* injected with PSCCAG-GFP (histological sections). Quantitative analysis Graph: mean±s.e.m. in 5 random fields per sample. Student's t-test, (NS: 10 non-significant). Scale bars: B-C=10um.

Changes/Problems:

As an initial attempt to complement a defective organ niche in *Fgfr2*^{cnull} mutants, we used pluripotent stem cells (PSCs) derived from an *Nkx2-1-GFP knockin* mouse as donor cells PSC$^{Nkx2\text{-}1\text{-}GFP}$ cultured in 2i-media condition (*9*). These cells express green fluorescent protein (GFP) from the *Nkx2-1* locus, thus marking all lung epithelial progenitors from their earliest stages. PSCs$^{Nkx2\text{-}1\text{-}GFP}$ were expected to respond to Fgf10 from the host to form the lungs (*10*). Among the 25 PSCs$^{Nkx2\text{-}1\text{-}GFP}$ injected into *Fgfr2*^{cnull}, WT or *Fgfr2* ^{hetero} blastocysts transferred to pseudo-pregnant mothers, 12 reached term. Of these, two showed respiratory distress, dying immediately at birth. The remaining 10 pups were sacrificed as 2-month old adults. Analysis of their lungs showed chimerism in 5 of these mice; GFP signals were nevertheless patchy and low, suggesting that the niche to be complemented was unlikely vacant as expected in *Fgfr2*^{cnull} mutants. Surprisingly, in embryos that died at birth, instead of agenesis, GFP+ donor-derived lungs were present in the thoracic cavity. Although uninflated and thus slightly smaller, these lungs had no obvious gross abnormalities suggestive of altered lobation or arrested branching morphogenesis (Fig.3). Morphometric analyses revealed that nearly 100% of the lung epithelium was comprised of GFP+ cells. The extensive overlap of GFP and nuclear Nkx2-1 signals further confirmed that PSCs$^{Nkx2\text{-}1\text{-}GFP}$ were able to complement with high efficiency a vacant endodermal niche in the *Fgfr2*^{cnull} hosts to undergo lung organogenesis (Fig. 3). Nevertheless, the chimeric lungs were immature. Airways branched and differentiated seemingly normally, but the alveolar saccules crucial for gas-exchange never formed. Caveolin1 is nearly absent in the distal epithelium, albeit Caveolin1 is widespread in the distal mesenchyme suggesting that AT1 cell differentiation did not occur (Fig. 3). Thus, complementation with PSCs$^{Nkx2\text{-}1\text{-}GFP}$ was inefficient in carrying out the final steps of lung maturation and functionally rescuing the respiratory failure of *Fgfr2*^{cnull} hosts. We reasoned this could have resulted from low developmental potential of PSCs$^{Nkx2\text{-}1\text{-}GFP}$ perhaps due the Nkx2-1 haploinsufficiency of this knockin line and/or a non-optimal protocol used to maintain these cells in culture (*11–13*). We are also addressing the potential epigenetic mechanism why a2i/VPA/LIF culture condition have the high frequency of functional PSCs that form high chimerism and high complementation (Now under the review of Nature Medicine).

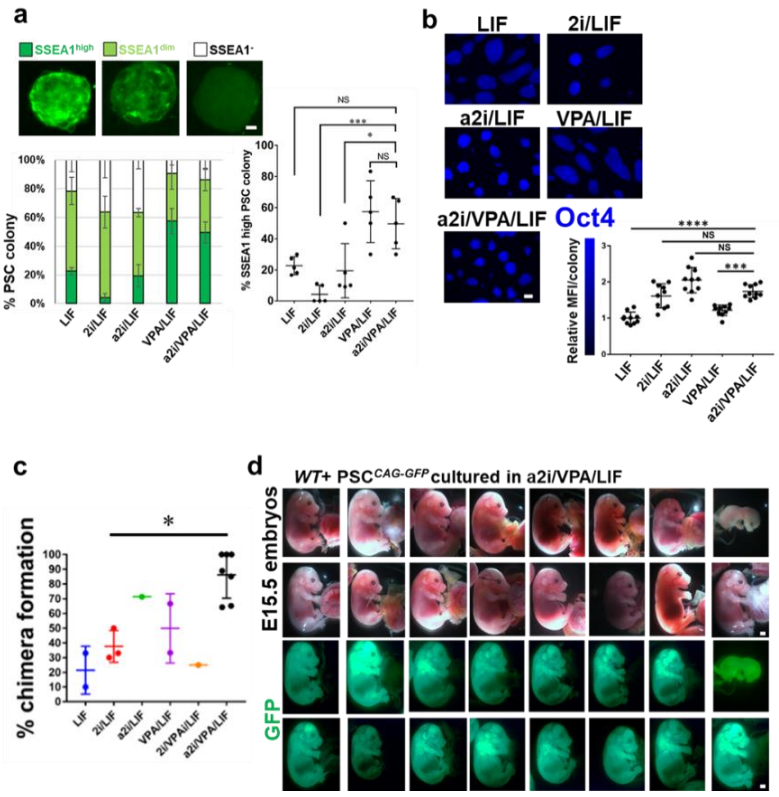

Fig. 10 Effect of a2i/VPA/LIF culture condition in PSC pluripotency and chimerism. (**a**) Classification of PSC colonies based on the SSEA1 expression levels by IF analyses. VPA/LIF and a2iVPA/LIF significantly yielded the highest percentage of SSEA1 high colonies. (n=3, 1-way ANOVA), (**b**) a2i /VPA/LIF yielded to significantly higher Oct4 levels (mean fluorescent intensity: MFI) compared to VPA/LIF (n=3, 1-way ANOVA), (**c**) The number of chimeric pups at P0/the number of transferred blastocysts after the transfer of blastocysts injected with each PSC-cultured in each condition. (d) High frequency of GFP-expressing chimera formation in WT embryos at E15.5 after the PSC$^{CAG\text{-}GFP}$ injection into WT blastocysts. ; statistically significant: ****p<0.0001, ***p<0.001, **p<0.01, *p<0.05, NS: statistically non-significant: p> 0.05.

In Aim2, although we expected to target lung buds under ultrasound echo guidance, we could not clearly observe the lung region. Therefore, we are planning to use embryos at later stages such as E11.5~E16.5 for the lung progenitor injections. Alternatively, we are also planning to generate transgenic mice that can label specifically lungs (Ex. Nkx2-1-Cre; Rosa ^{iRFP}) to optimize the ideal conditions for LBC injection as a survival surgery in the mouse because the lung buds are too small and invisible under ultrasound echo.

Products:

Pending publication (Nature Medicine, revision now).

Participants & Other Collaborating Organizations:

Munemasa Mori, MD, PhD	PI
Wellington V. Cardoso, MD, PhD	Other Significant Contributor – Mentorship (No Change)
Hiromitsu Nakauchi, PhD	Other Significant Contributor – Mentorship (No Change)
Darrell N. Kotton, MD	Other Significant Contributor – Mentorship (No Change)
Matthew Bacchetta, MD	Other Significant Contributor – Mentorship (No Change)
Ellen Ezratty, PhD	Contributor – Technical Guidance
Jennifer A. Danielsson, MD	Other Significant Contributor - Collaborator
Charles W. Emala, MD	Other Significant Contributor- Collaborator

Mayu Ota, MA Research Technician – Assists in modeling of iPS using genome-edited mouse/human iPS cells for generating functional lungs.

Special Reporting Requirements:
Nothing to Report

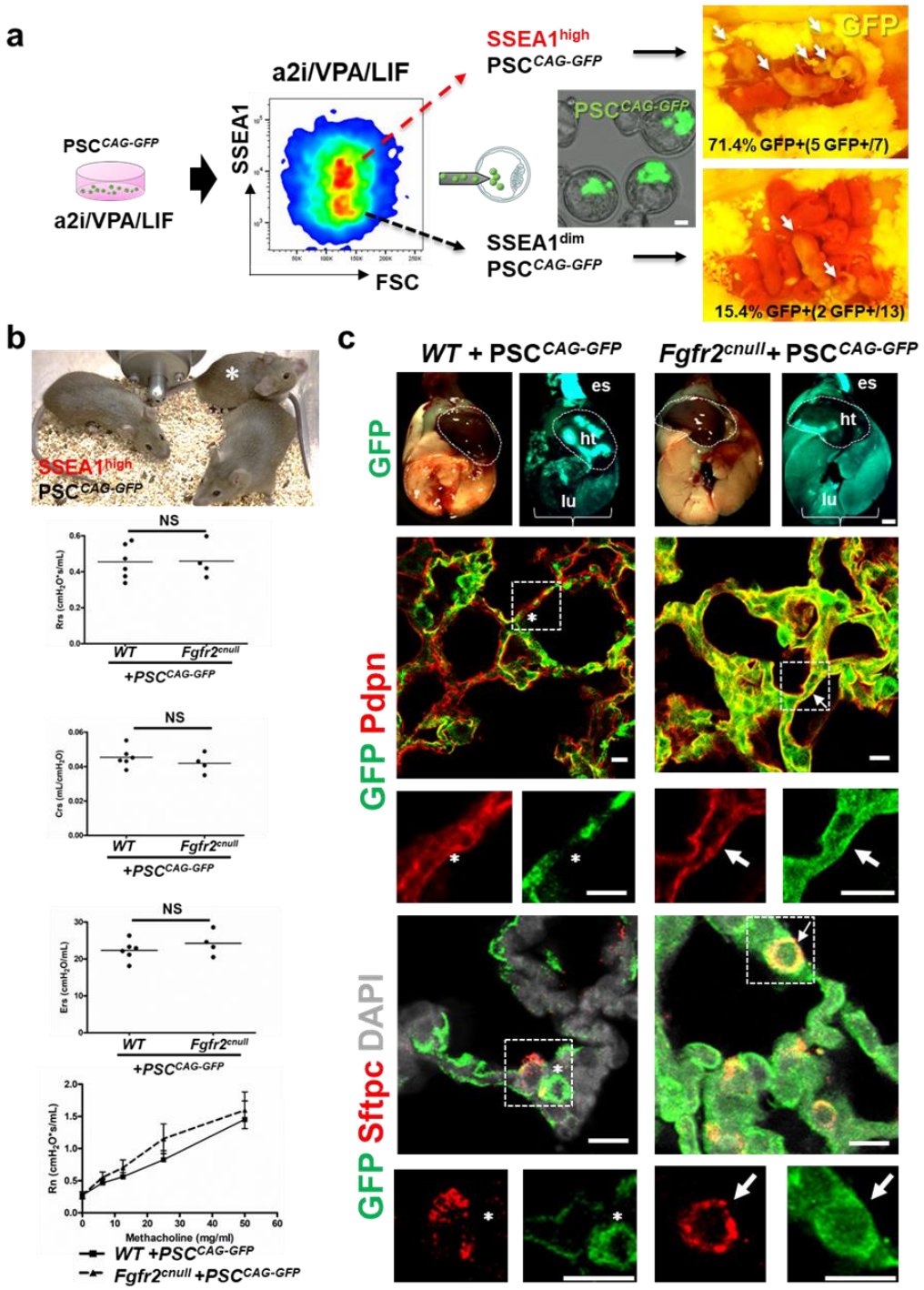

Figure 11. Generation of fully functional adult lungs in Fgfr2-deficient mice via CBC (**a**) Schematic of experimental design. a2i/VPA/LIF-treated PSC $^{CAG-GFP}$ sorted into SSEA1^{high} and SSEA1^{dim}; high frequency of chimera formation in neonatal WT pups injected with SSEA1 ^{high} compared to SSEA1^{dim} PSCs (representative litter; arrows: GFP in the skin) (**b**) Functional analysis of adult complemented mice. Top panel: adult Fgfr2^{cnull}+ PSC $^{CAG-GFP}$ (asterisk: *) and control WT + PSC $^{CAG-GFP}$ mice show no difference in activity or feeding behavior. Flexivent analysis of pulmonary function: no significant difference in baseline resistance of the respiratory system (Rrs), compliance (Crs), or elastance (Ers). Complemented adult Fgfr2^{cnull} and WT lungs respond similarly when challenged with increasing doses of Methacholine (Rn, the resistance of conducting airways). Student's t-test, NS: statistically non-significant (see methods). (c) Extensive GFP signals in postnatal day 80 adult lungs (lu, bracket) of Fgfr2cnull+ PSC $^{CAG-GFP}$ as compared with littermate control WT + PSC $^{CAG-GFP}$ (whole mounts). Note variable chimerism in the heart (ht), esophagus (es) and lungs of WT. Fgfr2^{cnull} + PSC $^{CAG-GFP}$ IF (right) showing GFP+ donor cells in nearly all the alveolar epithelium double-labeled with markers of alveolar type1 (Pdpn) and type2 (Sftpc) cells, compared with WT + PSCCAG-GFP (right). Each bottom panels in (c): boxed areas enlarged from top panel (arrows: GFP+marker+ cells; * marker+ alone). Scale bars: a: 10μm, c; top panel: 1mm, middle and bottom panels 10μm, respectively.

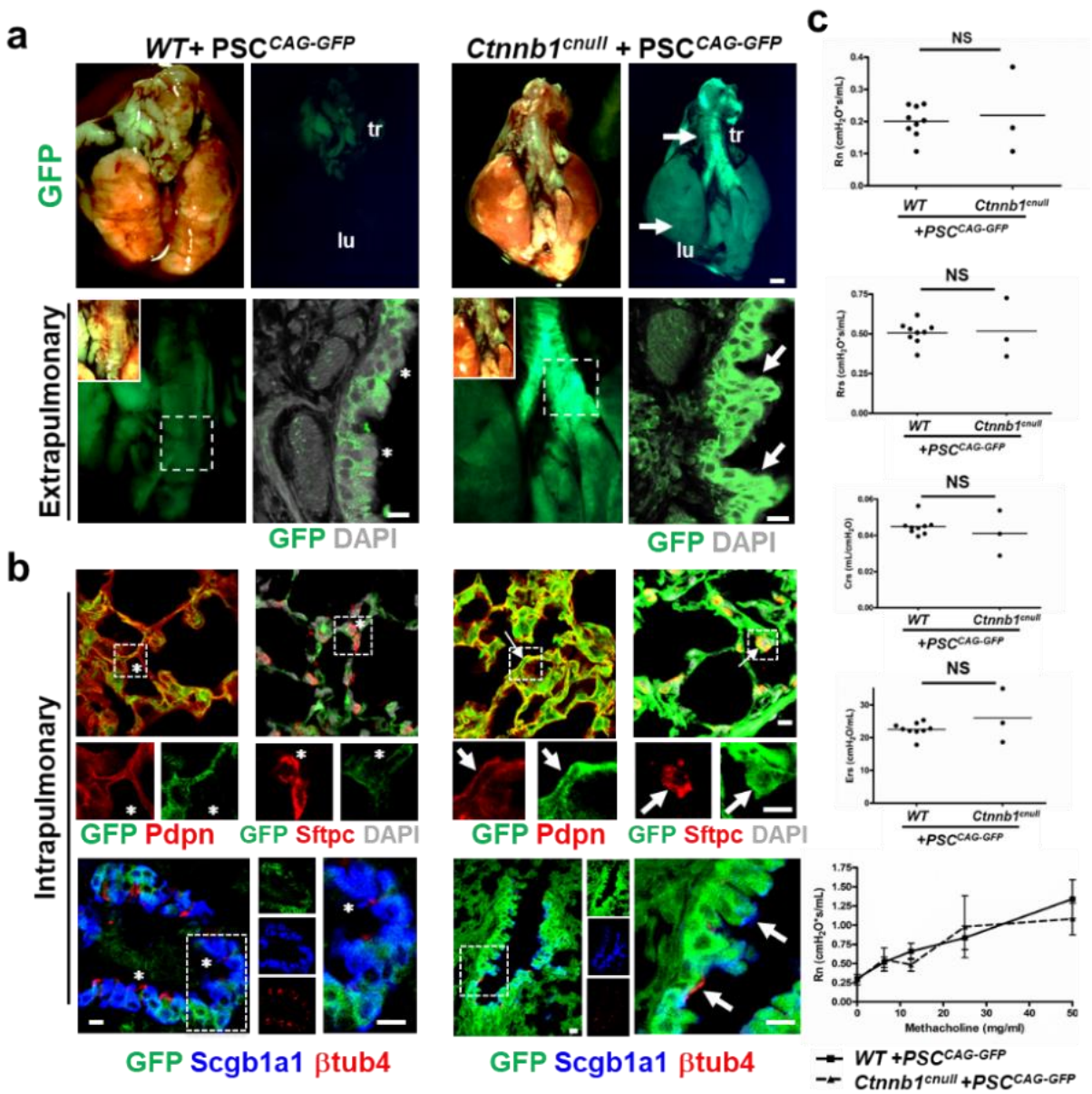

Fig. 12 CBC overcomes the inability to specify the early respiratory progenitors and generates trachea and functional lungs in Ctnnb1-deficient mice. Adult postnatal day 50 lungs and trachea from a2i/VPA/LIF-treated PSC$^{CAG-GFP}$ injected into the Ctnnb1^{cnull} (right) or control WT (left) blastocysts. (a) Whole mounts: extensive GFP signals (arrows) in the adult lung (lu) and trachea (tr) of the Ctnnb1^{cnull}+ PSC$^{CAG-GFP}$ chimeric mice contrasting with low signals of WT + PSC$^{CAG-GFP}$. Lower panels: IF confirming the strong GFP epithelial signals in the trachea and extrapulmonary bronchi of mutants, unlike WT (insets: areas depicted in squares). (b) Representative IF-Confocal image depicting GFP signals in alveolar type 1 (Pdpn+) and type 2 (Sftpc+)cells and intrapulmonary airway multiciliated (β-tubulin4) and secretory cells (Scgb1a1). Squared areas enlarged in small panels/single channels. Each bottom panels in (a-b): boxed areas enlarged from top panel (arrows: GFP+marker+ cells; * marker+ alone). (c) Flexivent analysis: pulmonary function in adult complemented WT and mutants (see methods). No significant change in any of the parameters (Rn, Rrs, Crs, Ers), including methacholine challenge in Ctnnb1^{cnull} + PSC$^{CAG-GFP}$ compared with WT + PSC$^{CAG-GFP}$. Student's t-test, NS: statistically non-significant. Scale bars: a (a top panel: 1mm, a bottom panel:10μm), b: 10μm, respectively.

Appendices

List of research outcomes:

1. **Publications:** Manuscript in review *Nature Medicine*: Generation of functional lungs via conditional blastocyst complementation.
2. **Patents:** pending (Columbia University Medical Center).
3. **Presentations:** Keystone Conference Invited Speaker (2019, Tahoe) Oral Presentation: “Cell Specification or Proliferation? Which Will Win for Organ Generation?”
4. **Development of resources:** Establishment of conditional blastocyst complementation technologies, efficient generation of functional mouse PSCs that forms lungs.

References:

1. K. Sekine *et al.*, Fgf10 is essential for limb and lung formation. *Nat. Genet.* **21**, 138–41 (1999).
2. F. G. Sala *et al.*, FGF10 controls the patterning of the tracheal cartilage rings via Shh. *Development*. **138**, 273–82 (2011).
3. L. De Moerlooze *et al.*, An important role for the IIIb isoform of fibroblast growth factor receptor 2 (FGFR2) in mesenchymal-epithelial signalling during mouse organogenesis. *Development*. **127**, 483–92 (2000).
4. N. Saiz, K. M. Williams, V. E. Seshan, A. K. Hadjantonakis, Asynchronous fate decisions by single cells collectively ensure consistent lineage composition in the mouse blastocyst. *Nat. Commun.* **7** (2016), doi:10.1038/ncomms13463.
5. K. S. Harris, Z. Zhang, M. T. McManus, B. D. Harfe, X. Sun, Dicer function is essential for lung epithelium morphogenesis. *Proc. Natl. Acad. Sci. U. S. A.* **103**, 2208–13 (2006).
6. K. Yu, Conditional inactivation of FGF receptor 2 reveals an essential role for FGF signaling in the regulation of osteoblast function and bone growth. *Development*. **130**, 3063–3074 (2003).
7. X. Xu *et al.*, Fibroblast growth factor receptor 2 (FGFR2)-mediated reciprocal regulation loop between FGF8 and FGF10 is essential for limb induction. *Development*. **125**, 753–765 (1998).
8. E. Arman, R. Haffner-Krausz, M. Gorivodsky, P. Lonai, Fgfr2 is required for limb outgrowth and lung-branching morphogenesis. *Proc. Natl. Acad. Sci.* **96**, 11895–11899 (1999).
9. Q.-L. Ying *et al.*, The ground state of embryonic stem cell self-renewal. *Nature*. **453**, 519–23 (2008).
10. T. a Longmire *et al.*, Efficient derivation of purified lung and thyroid progenitors from embryonic stem cells. *Cell Stem Cell*. **10**, 398–411 (2012).
11. M. Yagi *et al.*, Derivation of ground-state female ES cells maintaining gamete-derived DNA methylation. *Nature*. **548**, 224–227 (2017).
12. J. Choi *et al.*, Prolonged Mek1/2 suppression impairs the developmental potential of embryonic stem cells. *Nature*. **548**, 219–223 (2017).
13. H. Krude *et al.*, Choreoathetosis, hypothyroidism, and pulmonary alterations due to human NKX2-1 haploinsufficiency. *J. Clin. Invest.* **109**, 475–480 (2002).
14. M. Stadtfeld *et al.*, Aberrant silencing of imprinted genes on chromosome 12qF1 in mouse induced pluripotent stem cells. *Nature*. **465**, 175–181 (2010).
15. L. Weinberger, M. Ayyash, N. Novershtern, J. H. Hanna, Dynamic stem cell states: Naive to primed pluripotency in rodents and humans. *Nat. Rev. Mol. Cell Biol.* **17**, 155–169 (2016).
16. T. Furusawa, K. Ohkoshi, C. Honda, S. Takahashi, T. Tokunaga, Embryonic Stem Cells Expressing Both Platelet Endothelial Cell Adhesion Molecule-1 and Stage-Specific Embryonic Antigen-1 Differentiate Predominantly into Epiblast Cells in a Chimeric Embryo1. *Biol. Reprod.* **70**, 1452–1457 (2004).
17. A. Kretsovali, C. Hadjimichael, N. Charmpilas, Histone deacetylase inhibitors in cell pluripotency, differentiation, and reprogramming. *Stem Cells Int.* **2012** (2012), doi:10.1155/2012/184154.
18. A. M. Goss *et al.*, Wnt2/2b and beta-catenin signaling are necessary and sufficient to specify lung progenitors in the foregut. *Dev. Cell*. **17**, 290–8 (2009).

FEDERAL FINANCIAL REPORT

(Follow form instructions)

1. Federal Agency and Organizational Element to Which Report is Submitted	2. Federal Grant or Other Identifying Number Assigned by Federal Agency (To report multiple grants, use FFR Attachment)	Page	of
USA MED RESEARCH ACQ ACTIVITY	W81XWH-17-1-0139	1	1 pages

3. Recipient Organization (Name and complete address including Zip code)
Trustees of Columbia University in the City of New York
PO Box 29789, General Post Office, New York, NY 10087-9789

4a. DUNS Number	4b. EIN	5. Recipient Account Number or Identifying Number (To report multiple grants, use FFR Attachment)	6. Report Type	7. Basis of Accounting
62-188-9815	1135598093A7	GG012778	□ Quarterly □ Semi-Annual X Annual □ Final	X Cash □ Accrual

8. Project/Grant Period From: (Month, Day, Year)	To: (Month, Day, Year)	9. Reporting Period End Date (Month, Day, Year)
May 1, 2017	February 28, 2019	December 31, 2018

10. **Transactions**	Cumulative
(Use lines a-c for single or multiple grant reporting)	
Federal Cash (To report multiple grants, also use FFR Attachment):	
a. Cash Receipts	$275,597.51
b. Cash Disbursements	$285,868.58
c. Cash on Hand (line a minus b)	($10,271.07)
(Use lines d-o for single grant reporting)	
Federal Expenditures and Unobligated Balance:	
d. Total Federal funds authorized	$319,627.00
e. Federal share of expenditures	$285,868.58
f. Federal share of unliquidated obligations	$0.00
g. Total Federal share (sum of lines e and f)	$285,868.58
h. Unobligated balance of Federal funds (line d minus g)	$33,758.42
Recipient Share:	
i. Total recipient share required	$0.00
j. Recipient share of expenditures	$0.00
k. Remaining recipient share to be provided (line i minus j)	$0.00
Program Income:	$0.00
l. Total Federal program income earned	$0.00
m. Program income expended in accordance with the deduction alternative	$0.00
n. Program income expended in accordance with the addition alternative	$0.00
o. Unexpended program income (line l minus line m or line n)	$0.00

	a. Type	b. Rate	c. Period From	Period To	d. Base	e. Amount Charged	f. Federal Share
11. Indirect	Predetermined	60.0%	5/1/2017	12/31/2018	178,667.86	107,200.72	107,200.72
						0.00	0.00
Expense						0.00	0.00
				g. Totals:	178,667.86	107,200.72	107,200.72

12. *Remarks:*
Prepared by Douglas Liang, Senior Finance and Compliance Manager - Sponsored Projects Finance (SPF)

13. Certification: By signing this report, I certify that it is true, complete, and accurate to the best of my knowledge. I am aware that any false, fictitious, or fraudulent information may subject me to criminal, civil, or administrative penalties. (U.S. Code, Title 218, Section 1001)

a. Typed or Printed Name and Title of Authorized Certifying Official	c. Telephone (Area code, number and extension)
Anna Shchupak, Associate Director	212-854-1073
	d. Email address: DL2903@columbia.edu
b. Signature of Authorized Certifying Official	e. Date Report Submitted (Month, Day, Year): 18-Jan-2019
	14. Agency use only:

Standard Form 425
OMB Approval Number: 0348-0061
Expiration Date: 10/31/2011

Paperwork Burden Statement
According to the Paperwork Reduction Act, as amended, no persons are required to respond to a collection of information unless it displays a valid OMB Control Number. The valid OMB control number for this information collection is 0348-0061. Public reporting burden for this collection of information is estimated to average 1.5 hours per response, including time for reviewing instructions, searching existing data sources, gathering and maintaining the data needed, and completing and reviewing the collection of information. Send comments regarding the burden estimate or any other aspect of this collection of information, including suggestions for reducing this burden, to the Office of Management and Budget, Paperwork Reduction Project (0348-0061), Washington, DC 20503.